

Vertical distribution of particulate matter near a national highway and influence of roadside tree canopy: A drone/UAV based study

Ravish Dubey^a, Aditya Kumar Patra^{b,d,*}, Jayadev Joshi^c, Daniel Blankenberg^c, Nazneen^d, Abhishek Penchala^b, Xuhui Lee^a

^a Yale School of Environment, Yale University, New Haven, CT, 06511, USA

^b Department of Mining Engineering, Indian Institute of Technology Kharagpur, Kharagpur, India

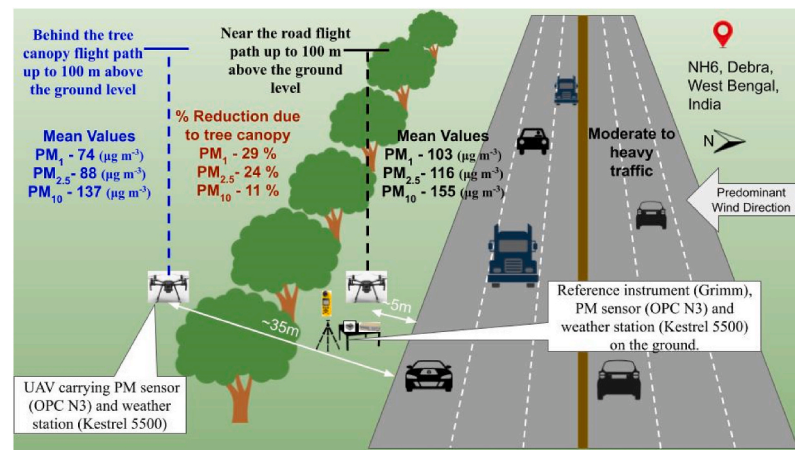
^c Lerner Research Institute, Cleveland Clinic, Cleveland, OH, 44195, USA

^d School of Environmental Science and Engineering, Indian Institute of Technology Kharagpur, Kharagpur, India

HIGHLIGHTS

- PM mass concentrations up to 100 m above ground level were measured using UAV.
- PM concentration increased with altitude followed by a decline for flights near the road.
- PM concentration decreased with altitude for flights behind the tree canopy.
- Tree canopy reduced PM₁, PM_{2.5} and PM₁₀ mass concentration by 29 %, 24 % and 11 %.
- A RF model predicted the UAV/ground PM concentration ratio with high accuracy.

GRAPHICAL ABSTRACT



ARTICLE INFO

Keywords:

Unmanned aerial vehicle (UAV)
 Particulate matter (PM)
 Open-highway
 Vertical PM concentration
 UAV/Ground concentration (U/G)
 Canopy cover

ABSTRACT

Measurement of PM near roadways has been of major interest due to high contributions of traffic to the overall PM. This paper presents the results from a study that used an unmanned aerial vehicle (UAV, also known as drones) platform to obtain measurements of PM and meteorological parameters up to 100 m above ground level near an open highway, and to understand the influence of tree canopy on the PM distribution. The study involved 42 flights over a period of two days, conducted adjacent to a national highway in India. The overall mean profile for flights conducted behind the tree canopy shows a decrease in PM mass concentrations with an increase in altitude. However, for the near-road flights, the PM concentrations tend to increase with altitude, followed by a gradual decline for a few flights. For the flights near the road, the results show that the mean values of PM₁ and PM_{2.5} mass concentrations at higher altitudes are 16% and 8% higher than the respective ground level concentrations. On the contrary, the mean PM₁₀ mass concentrations at higher altitudes are 6% lower than that at

* Corresponding author. Department of Mining Engineering, Indian Institute of Technology Kharagpur, Kharagpur, India.

E-mail address: akpatra@mining.iitkgp.ac.in (A.K. Patra).

<https://doi.org/10.1016/j.atmosenv.2024.120761>

Received 5 December 2023; Received in revised form 26 July 2024; Accepted 15 August 2024

Available online 21 August 2024

1352-2310/© 2024 Elsevier Ltd. All rights reserved, including those for text and data mining, AI training, and similar technologies.

the ground level. For the flights behind tree canopy, the results are different when compared to the flights near the road. The mean mass concentrations for all 3 p.m., PM_{2.5} and PM₁₀ particles at higher altitudes are 20%, 19% and 21% lower than the respective ground level measurements. Also, the PM₁, PM_{2.5} and PM₁₀ mass concentrations for the flight behind tree canopy cover are 29 %, 24 % and 11 % lower than the near-road flights respectively. The results also showed the concentrations behind the tree canopy remained low for the entire altitude of ~100 m.

1. Introduction

Traffic emissions contribute majorly to the particulate matter (PM) emissions in the environment (Das et al., 2015; Heydari et al., 2020; Kalaiarasan et al., 2018). Understanding the dispersion and distribution of PM emitted from traffic is crucial to assess their overall impact on human health as well as on the environment. Past studies have focused on evaluating the ground level distribution of particulate matter near public roadways (Barros et al., 2013; Tiitta et al., 2002)

However, to better understand the dispersion of PM, it is equally important to measure the PM concentrations in the vertical direction (Chilinski et al., 2016; Peng et al., 2015; Tao et al., 2016; Villa et al., 2016, 2017). Higher altitude measurements provide crucial information to evaluate the effects of temperature-inversions (Largeron and Staquet, 2016; Trinh et al., 2019; Wallace et al., 2010), urban heat islands (Fallmann et al., 2016; Sarrat et al., 2006) and influence of meteorology on PM dispersion (Tao et al., 2016).

As of 2019, the Ministry of Road Transport and Highways in India reported the total length of National Highways as 132,499 km. The rapid urbanization and expanding network of these highways mean that a significant portion of the population resides close to or in areas adjacent to National Highways. Thus, it is important to evaluate the distribution of PM near National Highways in India and evaluate the effectiveness of roadside tree canopy in reducing the exposure to PM. Ground level studies have shown that the tree canopy density affects the particulate matter distribution in the street canyons (Tiwari et al., 2019; Wang et al., 2020), however these studies do not provide information on distribution of PM above the tree height and overall effectiveness of the tree to reduce the PM exposure.

Vertical PM concentration profile studies can be crucial for a better estimate of the influence of roadside tree canopy cover (vegetation cover) on PM dispersion as against the ground-based studies (Deshmukh et al., 2018; Janhäll, 2015). Over the last couple of decades, researchers have adopted several techniques to measure the pollutant concentrations at higher altitudes. Some of the techniques include using multiple instruments/sensors at different heights of multi-storey building/meteorological tower, use of remote sensing techniques, balloons and aircrafts carrying PM measurement devices (Dubey et al., 2022c). With advances in the field of electronics and aerodynamics, Unmanned Aerial Vehicles (UAVs, also referred as drones) have been widely adopted in the last few years for various applications including aerial surveys and surveillance. A few studies have made use of UAVs as a platform to carry miniature PM measurement devices/sensors (Alvarado et al., 2017; Chilinski et al., 2018; Dubey et al., 2022b; Kuuluvainen et al., 2018; Peng et al., 2015; Villa et al., 2016, 2017). The availability of standard flight controllers in recent years has made it possible to automate flight planning and control, easy vertical take-off and landing, and an overall hassle-free operation without any or minimal requirement of manual intervention (Villa et al., 2016). One of the first major studies that deployed a UAV to measure the ultrafine particle number concentration near a major road was in Brisbane, Australia (Villa et al., 2017). Other past studies deployed UAV to measure the vertical as well as horizontal distribution of pollutants near roadways in semi-urban areas (Dubey et al., 2022b; Zheng et al., 2021).

Our study aimed to obtain a vertical distribution of particulate matter (PM) mass concentrations along with meteorological parameters up to a height of 100 m from the ground level using a UAV near a

National Highway in the eastern part of India. The research was designed to assess the impact of tree canopy cover on the distribution of particulate matter adjacent to an open highway, with UAV flights conducted both near the highway and behind the tree canopy. Additionally, we implemented a machine learning technique to predict PM mass concentrations at higher altitudes based on ground-level measurements. The hypothesis of the study is that higher altitude measurements would provide a comprehensive understanding of PM dispersion patterns and demonstrate the effectiveness of tree canopies in altering PM concentrations at various levels. This study is first of its kinds in its approach, to author's knowledge no major global study to date has deployed UAV-mounted sensors to measure high-altitude PM concentrations near highways and to examine the influence of roadside vegetation on PM dispersion. As such, the findings from this investigation are expected to be unique and provide novel insights into PM dispersion in traffic micro-environments near an open highway.

2. Methodology

The PM measurements and meteorological parameters were made using OPC N3 sensors from Alphasense and portable weather stations Kestrel 5500, respectively (detailed description in section 2.2.1 and 2.2.3). Identical instruments were placed on the ground level as well as on the UAV to get simultaneous measurements of PM concentrations and meteorological parameters. This was used to compare the higher altitude PM concentration against the ground level measurements. In addition to the sensors, the ground station also included a reference instrument, Grimm (model 1.108) (detailed description in section 2.2.2) to calibrate the PM sensors. The study design and experimental field campaign are explained further in section 2.3.

2.1. Measurement site and duration

The study was conducted adjacent to the National Highway 16 (NH 16), near Debra toll booth, West-Bengal, India, located at coordinates 22.39 °N, 87.52 °E. The roadway consisted of six lanes, three each on either side of the divider (Fig. S1). The site was chosen with no obstructions nearby and having open space to allow safe take-off and landing of the UAV. The tree canopy adjacent to the highway at the study site was ~15–20 m high and ~20–25 m wide. The open-highway site had no other major sources of PM except traffic. The traffic was moderate to heavy and consisted mainly of heavy vehicles and light passenger cars. The measurements were conducted for two days i.e. 11th and 13th January 2022.

2.1.1. Traffic count

Vehicle count data was obtained from the toll booth that records passing of any vehicle through the booth. The toll booth data categorized the vehicles into 8 categories viz. LMV (Light Motor Vehicle); TRUCK; LCV (Light Commercial Vehicle); MAV4AXE (Multi Axle Vehicle with 4 axles); MAV3AXE (Multi Axle Vehicle with 3 axles); BUS; MAV5AXE (Multi Axle Vehicle with 5 axles); MAV6AXE (Multi Axle Vehicle with 6 axles). For the ease of data analysis, we reduced these categories into one, Vehicle Count (VC; includes the sum of all the categories). The traffic count data used for the analysis is the sum of the vehicles during the past ~30 min prior to the flight take-off.

2.2. Instrumentation and sensor calibration

2.2.1. PM sensor

PM mass concentration was measured using OPC N3 sensors, manufactured by Alphasense, UK. It is a lightweight (105 g), compact (75 mm × 60 mm × 65 mm) optical particle counter which can detect particles in 24 size ranges, from 0.38 to 40 µm. The working principle of the sensor is based on the Mie scattering. The sensor uses an elliptical mirror and a dual-element photo-detector counts the particles. The sensor makes use of patented pumpless technology that allows the operation of the sensor in high PM concentration environments with minimum dust deposition and thus requires minimum maintenance (Alphasense, 2018). OPC N3 can be operated as a standalone PM monitor, however in that case the data stored is not time-stamped. To enable the data logging along with the time stamps, it must be operated either by connecting it to a laptop/computer and using it with the software provided by Alphasense or by operating it using a microcontroller/microprocessor. We used Raspberry Pi (model 3B) microprocessors to obtain and log the time-stamped data from the sensors. Raspberry Pi comes with several connectivity options such as SPI (Serial Peripheral Interface) pins and USB (Universal Serial Bus) ports. It is compact in size (85.60 mm × 56.5 mm × 17 mm) and weighs about 50 g, which makes it ideal to be mounted on a UAV alongside the PM sensor. The Raspberry was connected to the sensor via a USB port using a SPI to USB converter (can be procured from Alphasense). We used the python library provided by (Hagan et al., 2018) and modified it to log data continuously in CSV (Comma Separated Values) format (Dubey et al., 2022a). To ensure quality control and keep the potential sources of error minimal, the two OPC N3s used on the ground station and the UAV were newly procured. OPC N3 is an upgraded version of the sensor OPC N2. Studies have tested the performance of OPC N2 sensor against the standard instruments in controlled laboratory environments (Sousan et al., 2016), uncontrolled environments (Crilley et al., 2017; Dubey et al., 2022a) as well as high altitude environments simulated in the laboratory (Bezantakos et al., 2018). The results from these studies have shown that the sensor performs fairly accurately. The studies recommend on-site calibration of the sensor. Details of the sensor calibration for the present study are discussed in section 2.2.5.

2.2.2. Reference instrument

An aerosol spectrometer (Grimm, model 1.108), (hereon referred as Grimm) was used as a standard PM measuring device to calibrate the sensors. The instrument is widely regarded as one of the gold standards amongst the many optical principle-based instruments. The PM measurements from the Grimm have been found to be highly accurate in comparison with the FEM (Federal Equivalent Methods) (Burkart et al., 2010; Cheng, 2008). The proprietary software provided by Grimm was used to download the data and control the data logging parameters such as time interval etc.

2.2.3. Meteorological parameter measurements

The meteorological parameter measurements were made using a portable weather station manufactured by Nielsen-Kellerman (Model: Kestrel 5500), USA (Kestrel, 2019). The instrument is hereon referred as kestrel. Two identical kestrels were deployed on the ground as well as UAV to measure the meteorological parameters at a minimum logging interval of 2 s. Its compact size (6.5 cm × 7.5 cm × 22 cm), robust design and light weight (121 g) make it highly compatible for mounting on UAV. The proprietary software provided by Kestrel was used to download the data by connecting it to a laptop/computer. The portable weather station was also used to obtain the height of the UAV during the flight as it provides the altitude data by converting the barometric pressure into altitude.

2.2.4. UAV specifications and modifications

The UAV used in this study was a custom-made quadcopter that

offers a maximum payload capacity of 700 g. The UAV weighs a total 2 kg excluding the sensors (OPC N3) and weather station (Kestrel 5500). The flight time of the UAV is around 12 min without any payload. The UAV measures 450 mm diagonally and has carbon fiber propellers of 254 mm in size. The multi rotor motors powering the propellers are manufactured by T-motors (580 kV) with an ESC (Electronic Speed Controller) of 40 A (Ampere) supply. The UAV is powered by a 5200 mAh (milliampere-hour) LiPo (lithium polymer), 11.1 V, 3 cell battery. The autopilot used to operate and control the UAV was Pixhawk Q V5. All the UAV flights were planned and controlled using mission planner software from a laptop near the ground station. The software tracks the UAV status, battery health, altitude, latitude and longitude in real-time during the flight. Automated flights not only assisted in ease of operation but also ensured that all the flights followed the same path and the measurements were made at a constant uniform speed, thus avoiding any potential sources of human error. The UAV platform was customized to accommodate the PM sensor module and portable weather monitor to measure the PM mass concentrations as well as meteorological parameters. The PM sensor module was powered by the UAV batteries. Fig. 1 gives details of the sensor assembly along with the kestrel weather monitor. The sensors and micro-processor were placed at the center to achieve stable flights. Further, to avoid any measurement errors and to achieve PM measurements with minimal influence of the rotary wings of the UAV, a conductive sampling tube was attached to the inlet of the PM sensor with its other end ~50 cm above the rotary wings of the UAV. The rationale behind this is based on the CFD studies conducted earlier which showed that there is no influence of rotary wings on PM concentration beyond 50 cm above it (Alvarado et al., 2017). Also, based on our findings from the previous work, the conductive tube does not have a significant effect on the performance of the sensors (Dubey et al., 2022a).

2.2.5. Sensor calibration

The OPC N3 sensor used in this study is an updated version of OPC N2. Several past studies that have evaluated OPC N2 with the reference instrument have recommended that the sensor must be calibrated on-site with respect to a reference instrument (Crilley et al., 2017; Sousan et al., 2016). The findings from these studies have shown good performance of the sensors (Bezantakos et al., 2018). The US EPA has put forth criteria to evaluate the performance of low-cost sensors for supplemental and informational monitoring (US EPA, 2021). US EPA recommends the calibration of the sensors based on collocated measurements of the sensors with against a reference instrument. Our previous study, we extensively tested the performance of OPC-N2 and PM nova PM

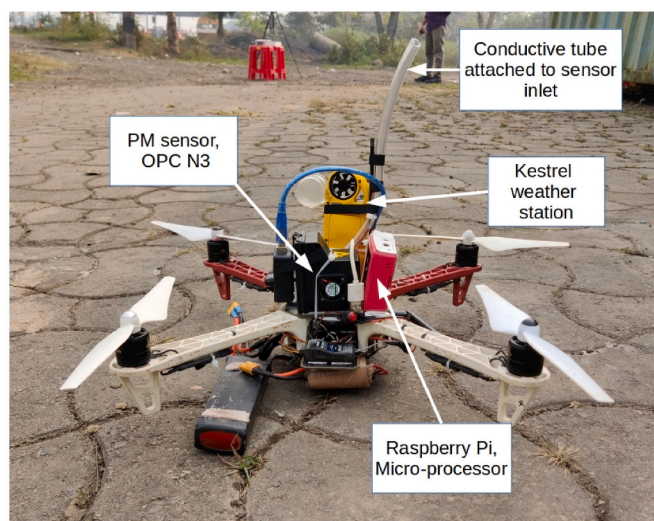


Fig. 1. UAV setup with sensor module and portable weather station.

sensors in different environments and conditions, including in traffic micro-environment. Based on the results of our previous work, OPC N2/N3 was found to perform better and also measures PM₁, PM_{2.5} and PM₁₀ concentrations simultaneously. However, results from other previous studies, including our previous work (Crilley et al., 2017; Dubey et al., 2022a; Sousan et al., 2016) suggested that the sensors must be calibrated via collocated measurements on-site before actual data collection. To achieve this, we measured the PM concentrations by operating OPC N3 sensors with Grimm as reference instrument for ~500 min at the site prior to actual measurements. The data from the measurement was used to evaluate the sensor performance using linear regression against reference instrument. The criteria set by the US EPA is a slope of 1 ± 0.3 , a y-intercept of $0 \pm 5 \mu\text{g m}^{-3}$, $R^2 \geq 0.7$ and RMSE values $< 7 \mu\text{g m}^{-3}$ for a linear regression between the sensor (as dependent variable) and reference instrument (as independent variable) (US EPA, 2021). The results of the sensor performance evaluation are shown in Table 1. The results show that the sensor performance was fairly accurate with high R^2 values. The sensors meet the US EPA performance criteria for most of the parameters. Further, the correction factors were obtained to express the PM concentrations measured by the sensors in terms of Grimm equivalent. These correction factors are shown in Fig. S2.

2.3. Description of field experimental plan

For safety, all the flights were operated manually for the first 5 m during the take-off and then switched into auto mode. The take-off point for all the near-road flights was at a distance of ~5 m from the edge of the highway. The UAV flights paths were vertical and up to a height of 100 m above the take off point. The ascent rate of the flight was controlled by the autopilot at a constant rate of 1 m s^{-1} . For the flights behind the tree canopy, the take-off point was at a distance of ~35 m from the edge of the highway. To understand the influence of tree canopy on PM distribution, flights behind the tree canopy were conducted immediately after the near-road flights. It is assumed that the overall distribution of the PM mass concentration did not change significantly during the time between behind the tree canopy flights and near-road flights. The ground level instruments were set at a perpendicular distance of ~5 m from the edge of the highway for near the road as well as behind the tree canopy flights. Fig. 2 shows a schematic representation of the experimental setup along with the flight path. The image was taken from another UAV which was intended to take pictures of the study. A total of 42 flights were conducted during two days of the experimental campaign. All the flight measurements were made between 10 a.m. and 5 p.m. IST (Indian Standard Time). Before the start of the experimental campaign, it was ascertained that all the instruments' and sensors' clocks are in synchronization.

The ground level setup included an OPC N3 sensor module, Grimm and kestrel 5500 to measure PM concentrations and meteorological parameters. An identical set of OPC N3 sensor module and kestrel 5500 were mounted on the UAV to measure the PM concentrations as well as meteorological parameters in the vertical direction. Data from the ground level OPC N3 sensor and the reference instrument Grimm was used to calibrate the data from the sensors. Corrections were applied to the data obtained from the sensors to get PM concentrations equivalent

Table 1

Evaluation of the OPC N3 for PM₁ and PM_{2.5} and PM₁₀ mass concentration with reference to Grimm.

PM size	Sensor evaluation parameters			
	Slope	Intercept	R ²	RMSE ($\mu\text{g m}^{-3}$)
PM ₁	0.94 ^a	-22.27	0.943 ^a	4.12 ^a
PM _{2.5}	1.46	-54.52	0.922 ^a	13.53
PM ₁₀	1.03 ^a	-15.05	0.57	46.75

^a meets the US EPA criteria.

to that of Grimm (Details in section 2.2.5).

2.4. Collected data analysis methods

The altitude data for the flights was obtained from the altitude sensor in Kestrel 5500. The minimum time interval for data logging in the Kestrel 5500 is 2 s. The data logging from the two OPC N3s was set at an interval of 2 s and synchronized using the time-stamps. As mentioned earlier, the ascent speed of the UAV was set to 1 m s^{-1} . Therefore, a 100 m high flight took ~100 s for the ascent, which led to ~50 data points per flight. The outliers were identified as the values beyond the $1.5 \times \text{IQR}$ (Interquartile Range) and were replaced with median values (Basu and Meckesheimer, 2007; Rousseeuw, 1991). Out of the 42 flights conducted over the span of two days, data from 22 flights was considered for analysis and the remaining 20 flights were discarded due to missing data from one or more instruments/sensors. For all the analysis, only the data between the altitudes 10 and 90 m from the UAV was considered. A rolling mean of 10 m interval was used for the analysis.

2.4.1. Random forest model

One of the main aims of the study was to develop a model to predict the PM mass concentrations at higher altitude based on the measurement of the ground level PM concentration and meteorological parameters. Random Forest (RF) is a meta-estimator that calculates a number of decision trees and performs analysis on the subsample of input data (Liaw and Wiener, 2002). A random forest model was developed to estimate the "UAV/Ground ratio" (ratio of mean values of higher altitude vs ground level PM mass concentrations). Ground level RH, wind speed, temperature and vehicle count and altitude were considered as independent variables to predict UAV/Ground ratio. Fig. 3 gives a schematic representation of the RF model parameters assigned along with the variables used. A rolling means of the UAV/Ground ratio values at 10 m intervals were considered for the model development and analysis. The depth of the tree for the RF model was adjusted to 7 with 100000 n_estimators. Time of the flight i.e. morning (M), afternoon (A) and evening (E) were considered as input to the RF model. However, like any other machine learning model, RF too requires data in the form of continuous variables for the regression model. A commonly used technique to convert the categorical data into continuous variables is One-Hot encoding (OHE). Binary numbers are used to convert the categorical data into continuous variables. For example, in our model the categorical variables are M, A, and E. Then, each unique category value is assigned with a binary number - M is "100", A - "010", E - "001" (Stepanov et al., 2020). The dataset from both the days was used to develop the model with 90 percent of data being used as training data and the rest of the 10 percent data used to evaluate the model performance.

3. Results and discussion

3.1. Meteorological conditions

Table 2 gives the descriptive statistics about the meteorological data obtained for ground level and the higher altitude measurements made by the UAV for all the flights. P-test results showed the mean values for higher altitude temperature (mean - Near road flights: 22.63 °C; Behind tree canopy flights: 21.78 °C) obtained by the UAV measurements were statistically significantly lower than ground level temperature (mean - Near road flights: 23.39 °C; Behind tree canopy flights: 22.98 °C). On the contrary, the mean value of relative humidity at higher altitude (mean: 77.21 %) was statistically higher than that at the ground level (mean: 75.26 %) for the near road flights. However, for the flights behind the tree canopy, the relative humidity values at higher altitudes (mean: 78.24 %) were found to be statistically indifferent from the ground-level mean values (mean: 77.45 %) based on the P-test results. The ground level wind speed during the flights (inclusive of near road and behind

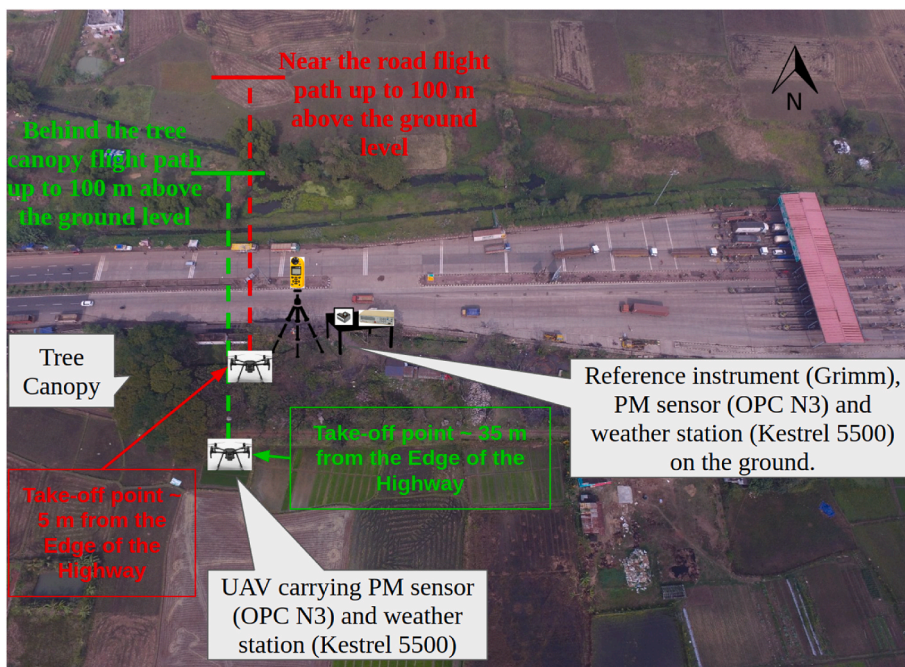


Fig. 2. Schematic representation of the experimental setup and design at the site (Not to scale).

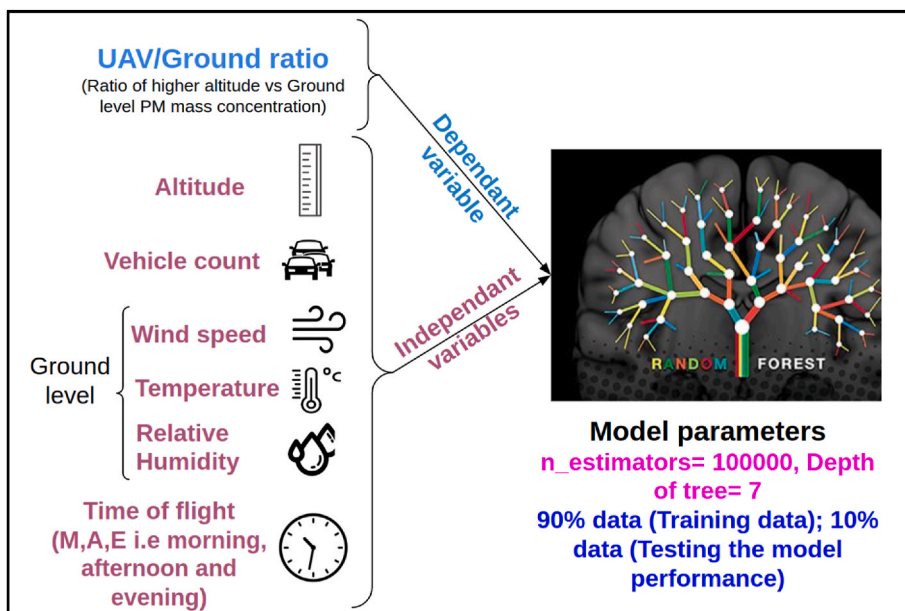


Fig. 3. Schematic diagram representing the Random Forest model parameters and variables.

Table 2
Descriptive statistics for the meteorological parameters for all the flights conducted over two days.

Parameters	Near Road				Behind Tree Canopy			
	Count (n)	Mean ± std	min	max	Count (n)	Mean ± std	min	max
Temperature ground (°C)	547	23.39 ± 3.10	19.40	29.00	578	22.98 ± 2.48	19.70	27.30
RH Ground (%)	547	77.21 ± 14.44	56.70	100.00	578	77.54 ± 11.29	61.50	100.00
Wind Speed ground (m s ⁻¹)	547	0.89 ± 0.64	0.00	2.60	578	0.81 ± 0.53	0.00	2.30
Temperature UAV (°C)	547	22.63 ± 3.26	17.60	28.30	578	21.78 ± 2.53	18.40	26.80
RH UAV(%)	547	75.26 ± 11.11	56.50	95.10	578	78.24 ± 9.56	59.80	95.70

Note- The ground level temperature and RH varied significantly from its corresponding values at higher altitudes ($p \leq 0.05$).

tree canopy flights) was in the range 0–2.6 m s⁻¹, with an overall mean value of 0.84 m s⁻¹, which shows that all the flights were conducted in the gentle breeze environment.

Fig. 4 shows the variation of temperature and RH with respect to altitude for all 22 flights. The flight number shows the order in which the flights were conducted. Temperature decreased with an increase in altitude for most of the flights, whereas the RH values were found to be increasing with an increase in altitude. The windrose diagrams show that the wind flow was from the north direction at the ground level for

most of the study duration. Therefore, all flights were conducted in the downwind direction of the highway (Figs. 2 and 4).

3.2. Vehicle count

Fig. S3 shows the variation of the sum of vehicle count ~30 min prior to the flight take-off for all the 22 flights. The vehicle count varied in the range of 149–246 vehicles (mean: 183 vehicles). For most of the study duration, the vehicle numbers increased as the day progressed. The

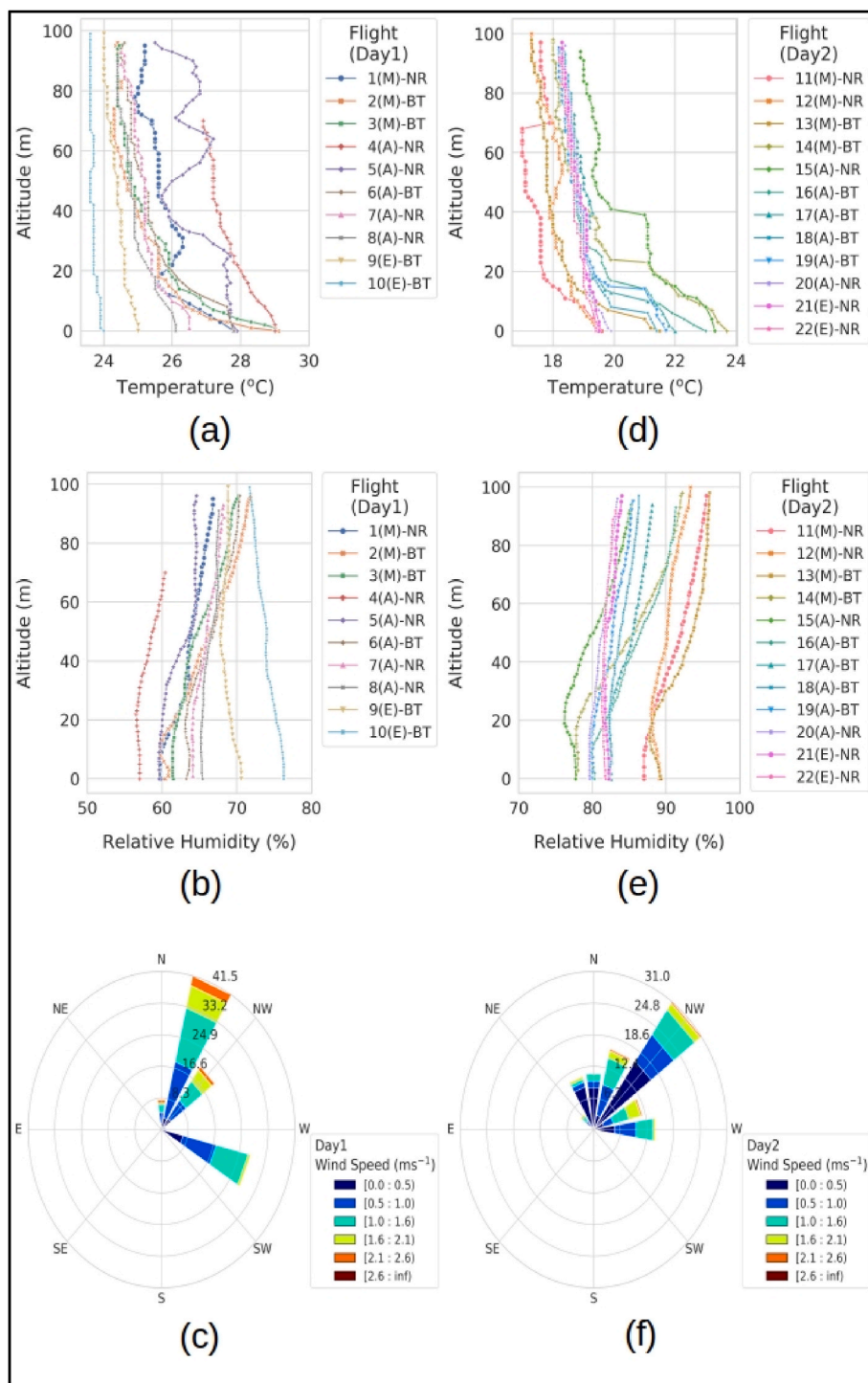


Fig. 4. Variation of temperature (a, d) and RH (b, e) with altitude, and windrose (c, f) at the ground level
 Note- (1) The X-axis scale is different for all the plots. (2) Suffix after the flight number denotes the time of the flight (M- Morning (Before 12pm), A-Afternoon(12-4 pm), E-Evening (After 4pm)), the letters NR represent the Near Road flights and BT represents flights Behind Tree canopy.

vehicle count was obtained from the database of the toll plaza.

3.3. PM mass concentration variation with altitude

Table 3 gives the descriptive statistics for PM mass concentration measurements at ground level and at higher altitudes for near the road and behind tree canopy flights. The p-test, or p-value test, is a statistical method used to determine the significance of results obtained from data analysis. If the p-value is less than 0.05 ($p < 0.05$), it suggests that the observed results are statistically significant, meaning there is less than a 5% probability that these results occurred by chance under the null hypothesis. In our study, we employed the p-value test to compare ground-level and higher altitude PM concentrations, aiming to determine if their differences were statistically significant. For the near road flights, the p-test results show that the PM_{10} (mean: $103.19 \mu\text{g m}^{-3}$) and $PM_{2.5}$ (mean: $116.11 \mu\text{g m}^{-3}$) mass concentrations at higher altitudes are significantly higher ($p \leq 0.05$) than the ground level concentrations (mean: $88.89 \mu\text{g m}^{-3}$ and $107.37 \mu\text{g m}^{-3}$ respectively). On the contrary, PM_{10} (mean: $164.54 \mu\text{g m}^{-3}$) and $PM_{2.5}$ mass concentrations at ground level is significantly higher ($p \leq 0.05$) than the concentrations at higher altitudes (mean: $155.17 \mu\text{g m}^{-3}$). This suggests that PM_{10} particles near the road settled close to the ground level and did not rise up to higher altitude during the study duration.

For the behind tree canopy flights, the results are different when compared to the near-road flights. The mass concentrations for all 3 p. m.₁ (mean: $73.81 \mu\text{g m}^{-3}$), $PM_{2.5}$ (mean: $88.07 \mu\text{g m}^{-3}$) and PM_{10} (mean: $137.38 \mu\text{g m}^{-3}$) particles at higher altitudes were significantly lower ($p \leq 0.05$) than that at the ground level measurements (mean: $91.56 \mu\text{g m}^{-3}$, $110.76 \mu\text{g m}^{-3}$ and $173.37 \mu\text{g m}^{-3}$ respectively).

The variation of PM mass concentration with respect to altitude for individual flights on both the days is shown in Fig. 5. The mean PM profile for near road and behind the tree canopy are shown separately. The flight numbers denote the order in which the flights were conducted and the letter after the flight number denotes the time of the flight (M-Morning (before 12 p.m.), A-Afternoon (12-4 pm), E-Evening (after 4 p.m.)).

The overall mean profile of the near-road flights shows an increase in the PM mass concentrations with the altitude for day 1 flights for all three particle sizes. For the day 2 flights near the road, the mean profile trend shows the mass concentrations increase with altitude followed by a gradual decline over 80 m. The onset of evening results in the formation of inversion, which leads to the trapping of the pollutants near the ground level, at a height of 50–60m, for a few of the evening and late afternoon flights on the second day of the measurements. Beyond it, from a height of ~80m, a decline in PM mass concentrations is observed. Studies have shown that PM concentrations usually decrease with the horizontal distance from the highway (Kärner et al., 2010; Zhu et al., 2002). The results from our study have shown the distribution of PM in vertical direction near the road and behind the tree canopy.

Table 3
Descriptive statistics of PM mass concentrations.

Parameters	Near Road				Behind Tree Canopy			
	Count (n)	Mean \pm std	min	max	Count (n)	Mean \pm std	min	max
Altitude (m)	547	48.38 \pm 27.50	0.00	100.00	578	48.46 \pm 28.28	0.00	99.00
PM_{10} ground ($\mu\text{g m}^{-3}$)	547	88.89 \pm 11.13 ^a	59.43	111.82	578	91.56 \pm 13.36 ^{aa}	67.77	124.34
$PM_{2.5}$ ground ($\mu\text{g m}^{-3}$)	547	107.37 \pm 29.12 ^b	63.47	156.15	578	110.76 \pm 24.39 ^{bb}	77.85	178.29
PM_{10} ground ($\mu\text{g m}^{-3}$)	547	164.54 \pm 29.12 ^c	100.65	267.17	578	173.37 \pm 31.06 ^c	126.49	268.01
PM_{10} UAV ($\mu\text{g m}^{-3}$)	547	103.19 \pm 21.05 ^a	38.21	176.77	578	73.81 \pm 9.39 ^{aa}	52.14	107.22
$PM_{2.5}$ UAV ($\mu\text{g m}^{-3}$)	547	116.11 \pm 31.38 ^b	50.50	220.60	578	88.07 \pm 16.73 ^{bb}	63.62	141.86
PM_{10} UAV ($\mu\text{g m}^{-3}$)	547	155.17 \pm 21.15 ^c	105.78	242.31	578	137.38 \pm 13.18 ^c	115.50	192.16

^a PM_{10} mass concentrations at ground level were significantly lower than that at UAV ($p \leq 0.05$).

^{aa} PM_{10} mass concentrations at ground level were significantly higher than that at UAV ($p \leq 0.05$).

^b $PM_{2.5}$ mass concentrations at ground level were significantly lower than that at UAV ($p \leq 0.05$).

^{bb} $PM_{2.5}$ mass concentrations at ground level were significantly lower than that at UAV ($p \leq 0.05$).

^c PM_{10} mass concentrations at ground level were significantly higher than that at UAV ($p \leq 0.05$).

Temperature was observed to decrease with altitude (Fig. 4) indicating effective vertical mixing. The PM concentration behind the tree canopy cover also decreased in a manner similar to the temperature profile. However, the PM concentration variations for flights near the road did not correlate strongly with the temperature profiles. The influence of ground-level meteorology on these observations is further discussed in Section 3.6. The overall mean profile for flights conducted behind the tree canopy shows a decrease in PM mass concentrations with an increase in altitude for both the days (Figs. 5 and 6). Section 3.4 provides a detailed discussion on the comparison between the near road and behind tree canopy flights.

3.4. Effect of tree canopy cover on PM distribution

The P-test results showed that the mean PM mass concentrations for PM_{10} , $PM_{2.5}$ and PM_{10} for behind tree canopy flights were significantly ($p < 0.05$) lower than the ones near the road (Table 3 and Fig. 6). The figure also shows the ground level PM mass concentrations from the measurements that were conducted at ~5 m from the edge of the highway for both, near the road and behind the tree canopy flights. The PM_{10} , $PM_{2.5}$, and PM_{10} mass concentrations for the flight behind tree canopy cover were 29 %, 24 %, and 11 % lower than the near road flights respectively (Table 3). The P-test results show that the tree canopy leads to a significant decrease ($p < 0.05$) in the PM mass concentrations. The findings from this study are similar to past studies that showed that the green infrastructure adjacent to the road leads to a reduction in PM_{10} , $PM_{2.5}$, and PM_{10} mass concentrations by 31 %, 17 %, and 15 % respectively (Abhijith and Kumar, 2019). However, the UAV-based measurements from the present study show that the PM mass concentrations remain low even up to ~100 m above the ground level for the flights behind the tree canopy cover in comparison to the near road flights (Fig. 6). The reduction in PM mass concentrations due to green infrastructure/canopy cover occurs through complex mechanisms that involve pollutant deposition and redistribution (Tiwari et al., 2019; Wang et al., 2020).

The results from our previous study (Dubey et al., 2022b) for the horizontal flights near an urban road without any trees had shown that the PM_{10} and $PM_{2.5}$ mass concentrations were 7 % and 11 % lower at a distance of 90 m than that at a 10 m distance from the edge of the urban road. PM_{10} did not show a significant ($p < 0.05$) difference in the mass concentrations. Even though the take-off distance for the behind tree canopy flights (~35 m) in the present study was less than half the distance of the horizontal flights (90 m) in the previous urban road study, the reduction in PM_{10} and $PM_{2.5}$ mass concentrations are higher. This suggests that the tree canopy cover, adjacent to the roads, leads to a significant reduction in the PM concentration level behind the canopy. The results from the UAV-based measurements from the present study show that the tree canopy cover led to a reduction in the PM mass concentration not only close to the ground but also up to several meters

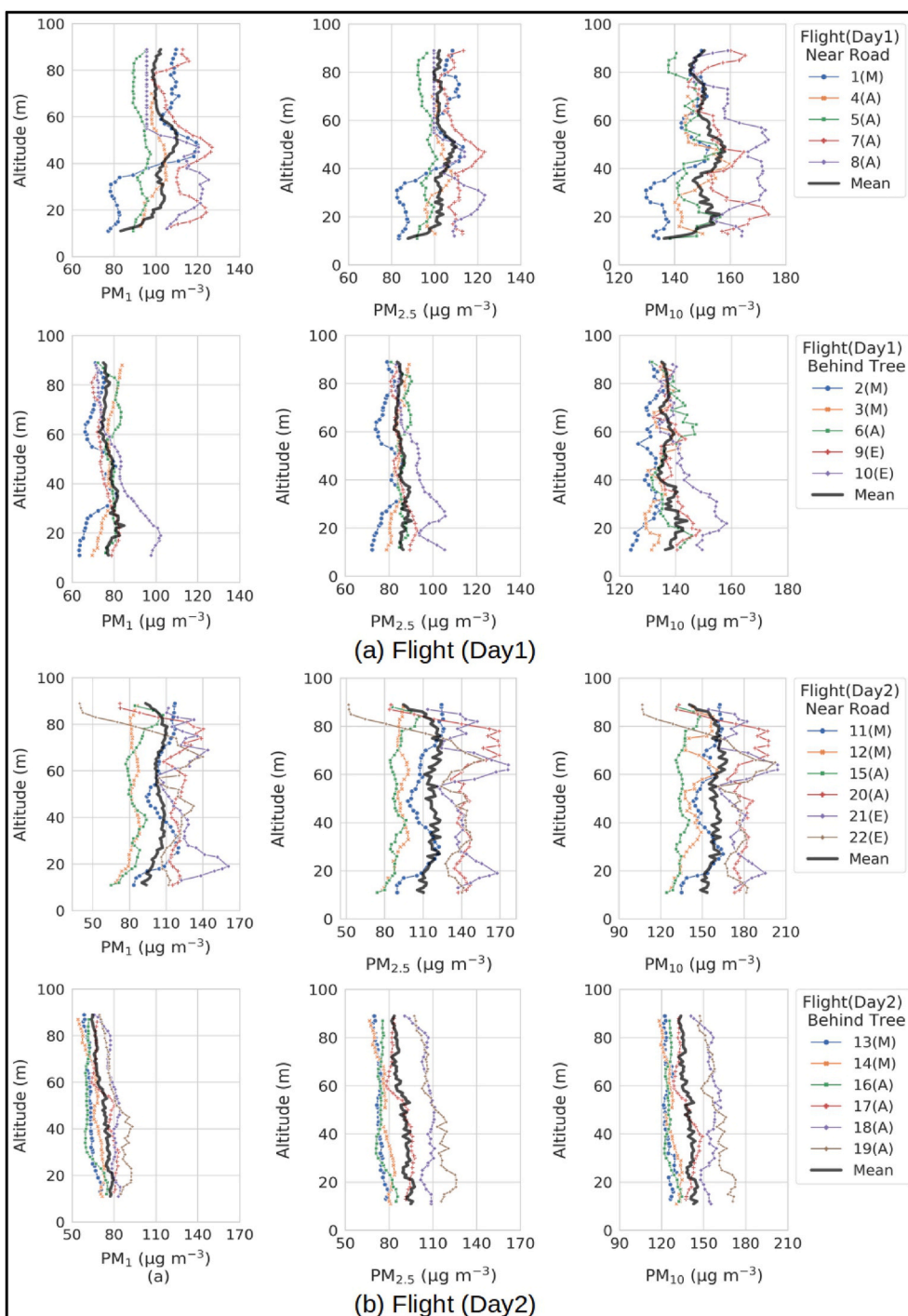


Fig. 5. PM mass concentration variation with altitude: (a) Day 1 (b) Day 2. Note: The X-axis scale is different for the plots. The letter after the flight number denotes the time of the flight (M- Morning (Before 12pm), A-Afternoon (12-4 pm), E- Evening (After 4pm)).

above the ground level. This is a major finding from this study and it shows that the UAV-based measurements of PM can provide crucial information leading to a better understanding of PM distribution in micro-environments.

3.5. Comparison of open highway and urban road PM distribution

This section discusses the differences in the vertical distribution of PM from our previous study near the urban road (Dubey et al., 2022b) and the present study near the open highway (near road flights only) and

highlights the major inferences from both the studies. UAV/Ground ratio (ratio of mean values of higher altitude vs ground level PM mass concentrations) of PM₁, PM_{2.5} and PM₁₀ for the near road scenario in case of the open highway are 1.16, 1.08 and 0.94, respectively (Table 3). These ratios are significantly higher for the open highway than urban roadway (0.93, 0.82 and 0.53 for PM₁, PM_{2.5} and PM₁₀ respectively (Dubey et al., 2022b)). All the ratios for our previous study near the urban road are <1 which suggests the ground level concentration is higher than the higher altitude concentrations. The possible explanation for this can be that the street canyons tend to restrict the PM dispersion

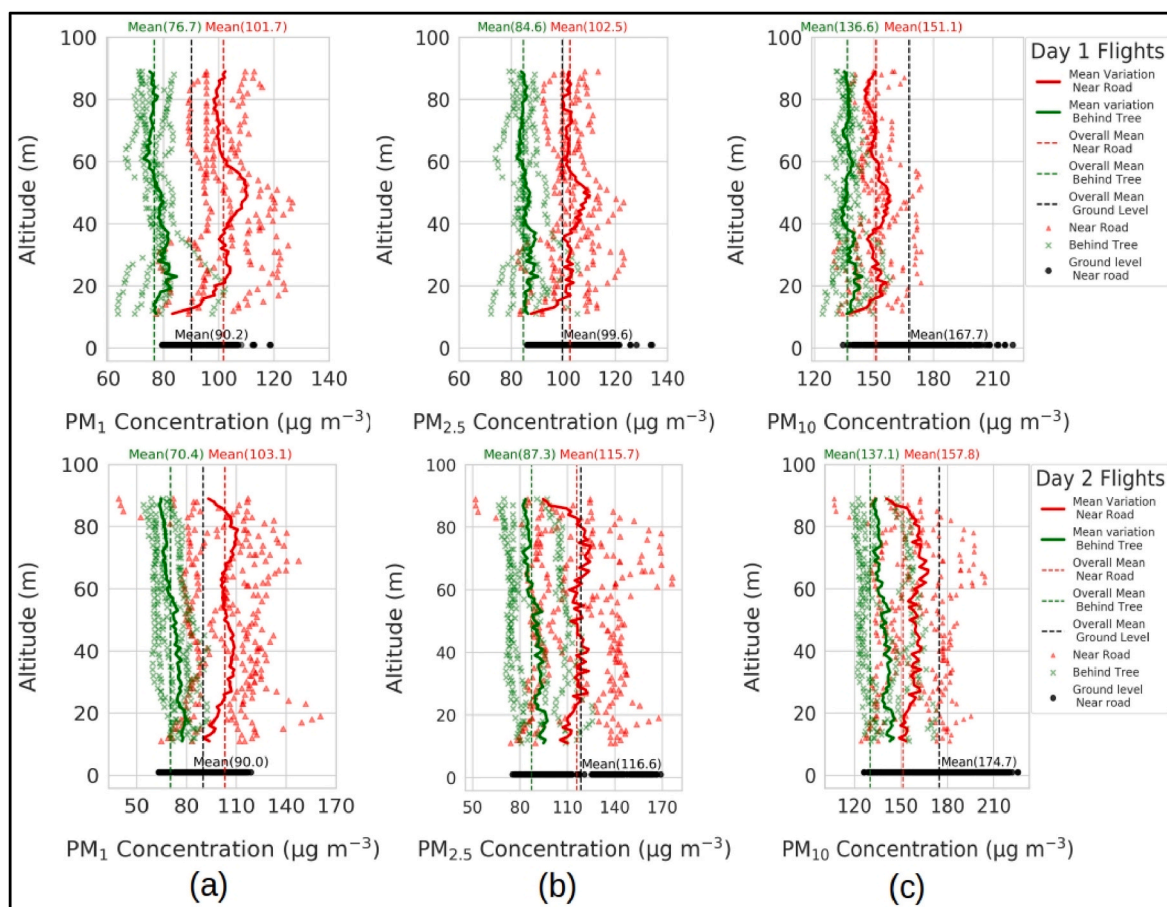


Fig. 6. Intercomparison of (a) PM₁, (b) PM_{2.5} and (c) PM₁₀ mass concentrations for the flights near road and behind tree canopy.

near urban roadways and ultimately lead to higher concentrations near the ground level (Chan and Kwok, 2000; Lv et al., 2021; Taseiko et al., 2009; Wang et al., 2021). In an urban street canyon, however, the exposure at higher altitudes is lower than the ground-level exposure levels.

The UAV/Ground ratio for the flights behind the tree canopy was 0.80, 0.81 and 0.79 (Table 3). In summary, the major inferences that can be drawn based on the inter-comparison of the two studies shows that that tree canopy cover greatly reduces PM exposure. Street canyons in the cities confine PM dispersion near ground level, suggesting staying on

higher floors is advisable in an urban environment. Conversely, PM distribution is uniform on open highways due to unrestricted airflow. Fig. 7 shows a schematic representation of the overall summary of the inferences that can be drawn from the UAV/Ground ratio near the urban roadway study and open highway study.

3.6. Random forest model evaluation

The random forest (RF) model was developed for flights near the road using the parameters discussed earlier in section 2.4.1. The

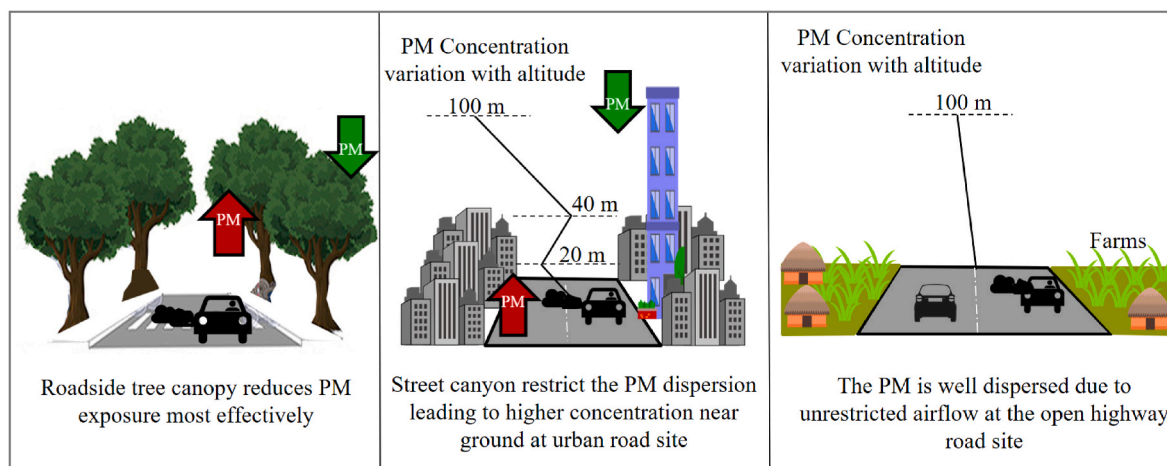


Fig. 7. Inferences from the UAV/Ground ratio of PM measurements near urban road and open highway.

Table 4
RF model performance metrics for UAV/Ground concentration predictions.

PM Size	Model evaluation parameters	
	R ²	RMSE
PM ₁	0.93	0.03
PM _{2.5}	0.94	0.03
PM ₁₀	0.90	0.05

performance of the RF model for the 10% test data is shown in Table 4. The high R² values (0.90–0.94) and low root mean squared error (RMSE) (0.03–0.05) values suggest that the model performed reasonably well.

Fig. 8 shows the variation between the actual and predicted UAV/Ground concentration ratio for the 10% test data for the flights near the road. The results show that the values predicted by the model are close to the actual values. The significance of the variables ground level temperature, RH and wind speed expressed as mean (all three particle sizes) percentage of feature importance were found to be 32.33%, 25.33% and 11.33% respectively. Mean percentage of the feature importance for altitude was found to be 22.33%. The performance metrics and the observations show that the RF model was accurate to get the UAV/Ground concentration for the near-road flights based on the ground-level parameters. The Random Forest model was developed following a methodology similar to our previous study (Dubey et al., 2022b), which involved vertical UAV measurements in an urban environment. The primary objective of the model was to predict higher altitude concentrations based solely on ground-level measurements. Our earlier study demonstrated promising performance from the model. To validate its efficacy, we conducted cross-validation using data from the open highway study, revealing that the technique yielded fairly accurate results across diverse study settings.

3.7. Limitations and uncertainties

The OPC N3 sensors employ a small fan to direct particles towards the detector, unlike costlier PM monitoring instruments equipped with an internal pump. The functioning of this fan may be susceptible to dust accumulation, potentially impacting measurements. To mitigate this risk, we utilized newly acquired OPC N3 sensors and ensured smooth

operation of the fan before each take-off. For more comprehensive details on the effect of wind, temperature, humidity and inter-comparison with other PM sensor we recommend to refer our previous study with detailed evaluation of performance of OPC N2/N3 (Dubey et al., 2022a).

Due to uncertainties over drone laws and regulations in India, we were granted permission by the toll management at Debra, West Bengal, to carry out our study for a limited period of time. We recognize that extending this study over various seasons and meteorological conditions would deepen our understanding of these factors' influences. The results from our study on the distribution of PM near open highway may vary from season to season. More studies are required across different seasons to better evaluate the influence of tree canopies on PM distribution.

4. Conclusions

The paper presented a UAV system consisting of PM and meteorological sensors to get vertical concentration profile of different PM sizes up to 100 m above the ground level, near a major national highway in India. The study also highlighted a unique and first-of-its-kind application of UAV-based measurements to understand the effect of tree canopy on PM distribution. The overall mean profile for flights conducted behind the tree canopy indicates that PM mass concentrations decrease with increasing altitude on both days. Conversely, for the near-road flights, PM concentrations generally increase with altitude up to mid-level altitudes or remain constant. However, a few flights did exhibit a decline in PM concentrations at higher altitudes, reaching levels similar to those observed in the flights behind the tree canopy. The findings from measurements near the open highway indicate that tree canopy cover alters PM mass concentration not only near ground level but also several meters above, resulting in an overall reduction in PM₁, PM_{2.5}, and PM₁₀ concentrations by 29%, 24%, and 11%, respectively. The comparative analysis between our earlier study conducted in urban settings and the current study along open highways highlights distinct patterns in particulate matter (PM) distribution. In urban environments, street canyons trap PM near the ground level, thereby limiting its dispersion. On the contrary, PM distribution along open highways is more uniform, benefiting from unrestricted airflow that allows particles to disperse more freely.

The study developed a relationship between the ground-level

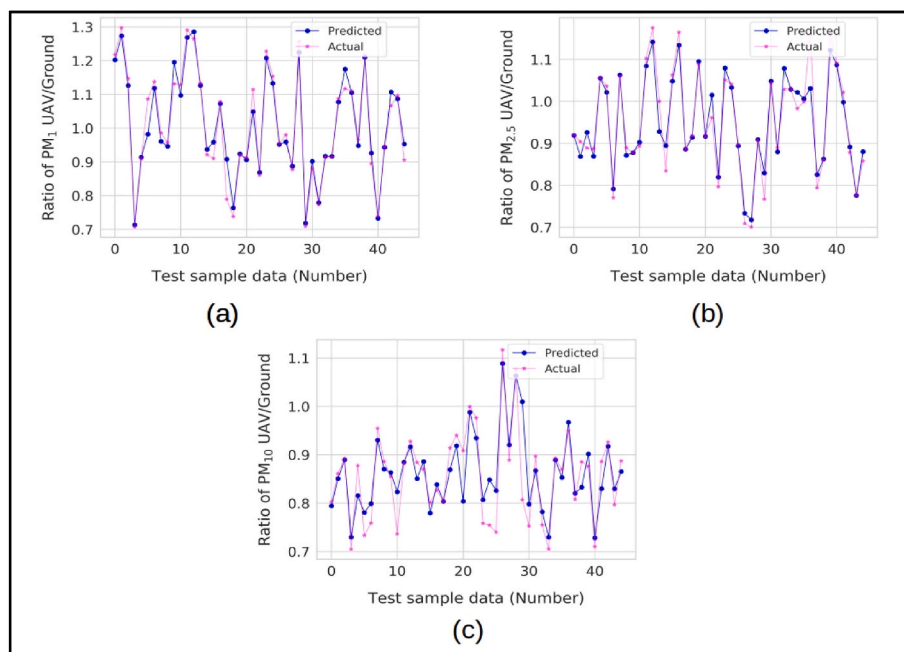


Fig. 8. Actual vs predicted ratio of UAV/Ground mass concentrations using RF model for (a) PM₁, (b) PM_{2.5} and (c) PM₁₀.

concentration of PM with concentrations at different altitudes for the flights near the road using an advanced machine learning algorithm named random forest. This can be used for predicting concentrations at different altitudes from the ground base measurements when the UAV-based measurements are not feasible. Based on these results, we recommend maintaining existing tree canopy cover along highways and initiating replanting efforts on those sections of Indian highways where trees were removed for the widening of highways. This strategy will help mitigate particulate matter concentrations and improve overall environmental health. We believe that the real-time vertical measurements of PM in a traffic environment are essential to understand the PM formation and distribution.

Our findings have shown that UAV-based vertical measurements of PM offer several advantages such as high resolution, flexibility of flight path, maneuverability, and hovering capability. UAVs will become the most widely adopted technique to get the vertical profile of pollutants, especially in micro-environments. More such studies must be carried out in different environments to better understand the vertical distribution of pollutants. Future studies may involve longer flight durations to obtain adequate samples for pollutant characterization, which can be ultimately used for source identification of PM at higher altitudes. With long flight duration, improved mission safety, flight repeatability due to improving autopilots, reduced operational costs as compared to manned aircrafts, and availability of low-cost sensors, UAV technology presents a promising solution for air quality measurement in the lower troposphere.

CRedit authorship contribution statement

Ravish Dubey: Writing – original draft, Visualization, Methodology, Investigation, Formal analysis, Data curation, Conceptualization. **Aditya Kumar Patra:** Writing – review & editing, Validation, Supervision, Resources, Project administration, Methodology, Funding acquisition, Conceptualization. **Jayadev Joshi:** Writing – review & editing, Formal analysis, Data curation. **Daniel Blankenberg:** Writing – review & editing, Supervision. **Nazneen:** Investigation, Data curation. **Abhishek Penchala:** Investigation, Data curation. **Xuhui Lee:** Writing – review & editing, Supervision.

Declaration of competing interest

The authors declare that they have no known competing financial interests or personal relationships that could have appeared to influence the work reported in this paper.

Data availability

Data will be made available on request.

Appendix A. Supplementary data

Supplementary data to this article can be found online at <https://doi.org/10.1016/j.atmosenv.2024.120761>.

References

- Abhijith, K.V., Kumar, P., 2019. Field investigations for evaluating green infrastructure effects on air quality in open-road conditions. *Atmos. Environ.* 201, 132–147. <https://doi.org/10.1016/j.atmosenv.2018.12.036>.
- Alphasense, 2018. Alphasense OPC N3 [WWW Document]. URL. <http://www.alphasense.com/index.php/products/optical-particle-counter/>, 11.6.20.
- Alvarado, M., Gonzalez, F., Erskine, P., Cliff, D., Heuff, D., 2017. A methodology to monitor airborne PM10 dust particles using a small unmanned aerial vehicle. *Sensors* 17. <https://doi.org/10.3390/s17020343>.
- Barros, N., Fontes, T., Silva, M.P., Manso, M.C., 2013. How wide should be the adjacent area to an urban motorway to prevent potential health impacts from traffic emissions? *Transport. Res. Pol. Pract.* 50, 113–128. <https://doi.org/10.1016/j.tra.2013.01.021>.
- Basu, S., Meckesheimer, M., 2007. Automatic outlier detection for time series: an application to sensor data. *Knowl. Inf. Syst.* 11, 137–154. <https://doi.org/10.1007/s10115-006-0026-6>.
- Bezantakos, S., Schmidt-Ott, F., Biskos, G., 2018. Performance evaluation of the cost-effective and lightweight Alphasense optical particle counter for use onboard unmanned aerial vehicles. *Aerosol. Sci. Technol.* 52, 385–392. <https://doi.org/10.1080/02786826.2017.1412394>.
- Burkart, J., Steiner, G., Reischl, G., Moshhammer, H., Neuberger, M., Hitzemberger, R., 2010. Characterizing the performance of two optical particle counters (Grimm OPC1.108 and OPC1.109) under urban aerosol conditions. *J. Aerosol Sci.* 41, 953–962. <https://doi.org/10.1016/j.jaerosci.2010.07.007>.
- Chan, L.Y., Kwok, W.S., 2000. Vertical dispersion of suspended particulates in urban area of Hong Kong. *Atmos. Environ.* 34, 4403–4412. [https://doi.org/10.1016/S1352-2310\(00\)00181-3](https://doi.org/10.1016/S1352-2310(00)00181-3).
- Cheng, Y.-H., 2008. Comparison of the TSI Model 8520 and Grimm Series 1.108 portable aerosol instruments used to monitor particulate matter in an iron foundry. *J. Occup. Environ. Hyg.* 5, 157–168. <https://doi.org/10.1080/15459620701860867>.
- Chiliński, M.T., Markowicz, K.M., Kubicki, M., 2018. UAS as a support for atmospheric aerosols research: case study. *Pure Appl. Geophys.* 175, 1–18. <https://doi.org/10.1007/s00024-018-1767-3>.
- Chilinski, M.T., Markowicz, K.M., Markowicz, J., 2016. Observation of vertical variability of black carbon concentration in lower troposphere on campaigns in Poland. *Atmos. Environ.* 137, 155–170. <https://doi.org/10.1016/j.atmosenv.2016.04.020>.
- Crilly, L.R., Shaw, M., Pound, R., Kramer, L.J., Price, R., Young, S., Lewis, A.C., Pope, F.D., 2017. Evaluation of a low-cost optical particle counter (Alphasense OPC-N2) for ambient air monitoring. *Atmos. Meas. Tech. Discuss* 1–24. <https://doi.org/10.5194/amt-2017-308>.
- Das, R., Khezri, B., Srivastava, B., Datta, S., Sikdar, P.K., Webster, R.D., Wang, X., 2015. Trace element composition of PM2.5 and PM10 from Kolkata – a heavily polluted Indian metropolis. *Atmos. Pollut. Res.* 6, 742–750. <https://doi.org/10.5094/APR.2015.083>.
- Deshmukh, P., Isakov, V., Venkatram, A., Yang, B., Zhang, K.M., Logan, R., Baldauf, R., 2018. The effects of roadside vegetation characteristics on local, near-road air quality. *Air Qual. Atmos. Health* 12, 1–12. <https://doi.org/10.1007/s11869-018-0651-8>.
- Dubey, R., Patra, A.K., Joshi, J., Blankenberg, D., Kolluru, S.S.R., Madhu, B., Raval, S., 2022a. Evaluation of low-cost particulate matter sensors OPC N2 and PM Nova for aerosol monitoring. *Atmos. Pollut. Res.* 101335 <https://doi.org/10.1016/j.apr.2022.101335>.
- Dubey, R., Patra, A.K., Joshi, J., Blankenberg, D., Nazneen, 2022b. Evaluation of vertical and horizontal distribution of particulate matter near an urban roadway using an unmanned aerial vehicle. *Sci. Total Environ.* 836, 155600 <https://doi.org/10.1016/j.scitotenv.2022.155600>.
- Dubey, R., Patra, A.K., Nazneen, 2022c. Vertical profile of particulate matter: a review of techniques and methods. *Air Qual. Atmos. Health*. <https://doi.org/10.1007/s11869-022-01192-1>.
- Fallmann, J., Forkel, R., Emeis, S., 2016. Secondary effects of urban heat island mitigation measures on air quality. *Atmos. Environ.* 125, 199–211. <https://doi.org/10.1016/j.atmosenv.2015.10.094>.
- Hagan, D., Tolmie, A., Trochim, J., 2018. py-opc: operate the Alphasense OPC-N2 from a raspberry pi or other popular microcontrollers/microcomputers. *J. Open Source Softw.* 3, 782.
- Heydari, S., Tainio, M., Woodcock, J., de Nazelle, A., 2020. Estimating traffic contribution to particulate matter concentration in urban areas using a multilevel Bayesian meta-regression approach. *Environ. Int.* 141, 105800 <https://doi.org/10.1016/j.envint.2020.105800>.
- Janhäll, S., 2015. Review on urban vegetation and particle air pollution – deposition and dispersion. *Atmos. Environ.* 105, 130–137. <https://doi.org/10.1016/j.atmosenv.2015.01.052>.
- Kalaiarasan, G., Balakrishnan, R.M., Sethunath, N.A., Manoharan, S., 2018. Source apportionment studies on particulate matter (PM10 and PM2.5) in ambient air of urban Mangalore, India. *J. Environ. Manag.* 217, 815–824. <https://doi.org/10.1016/j.jenvman.2018.04.040>.
- Karner, A.A., Eisinger, D.S., Niemeier, D.A., 2010. Near-roadway air quality: synthesizing the findings from real-world data. *Environ. Sci. Technol.* 44, 5334–5344. <https://doi.org/10.1021/es100008x>.
- Kestrel, 2019. Kestrel 5500 handheld weather station. <https://kestrelmeters.com> (accessed on 4 January 2022).
- Kuuluvainen, H., Poikkimäki, M., Järvinen, A., Kuula, J., Irjala, M., Dal Maso, M., Keskinen, J., Timonen, H., Niemi, J.V., Rönkkö, T., 2018. Vertical profiles of lung deposited surface area concentration of particulate matter measured with a drone in a street canyon. *Environ. Pollut.* 241, 96–105. <https://doi.org/10.1016/j.envpol.2018.04.100>.
- Largerone, Y., Staquet, C., 2016. Persistent inversion dynamics and wintertime PM10 air pollution in Alpine valleys. *Atmos. Environ.* 135, 92–108. <https://doi.org/10.1016/j.atmosenv.2016.03.045>.
- Liaw, A., Wiener, M., 2002. Classification and regression by random Forest. *R. News* 2, 18–22.
- Lv, W., Wu, Y., Zhang, J., 2021. A review on the dispersion and distribution characteristics of pollutants in street canyons and improvement measures. *Energies* 14, 6155. <https://doi.org/10.3390/en14196155>.
- Peng, Z.-R., Wang, D., Wang, Z., Gao, Y., Lu, S., 2015. A study of vertical distribution patterns of PM2.5 concentrations based on ambient monitoring with unmanned aerial vehicles: a case in Hangzhou, China. *Atmos. Environ.* 123, 357–369. <https://doi.org/10.1016/j.atmosenv.2015.10.074>.

- Rousseeuw, P.J., 1991. Tutorial to robust statistics. *J. Chemom.* 5, 1–20. <https://doi.org/10.1002/cem.1180050103>.
- Sarrat, C., Lemonsu, A., Masson, V., Guedalia, D., 2006. Impact of urban heat island on regional atmospheric pollution. *Atmos. Environ.* 40, 1743–1758.
- Sousan, S., Koehler, K., Hallett, L., Peters, T.M., 2016. Evaluation of the Alphasense optical particle counter (OPC-N2) and the Grimm portable aerosol spectrometer (PAS-1.108). *Aerosol Sci. Technol.* 50, 1352–1365. <https://doi.org/10.1080/02786826.2016.1232859>.
- Stepanov, N., Alekseeva, D., Ometov, A., Lohan, E.S., 2020. Applying machine learning to LTE traffic prediction: comparison of bagging, random forest, and SVM. In: 2020 12th International Congress on Ultra Modern Telecommunications and Control Systems and Workshops (ICUMT). Presented at the 2020 12th International Congress on Ultra Modern Telecommunications and Control Systems and Workshops (ICUMT), IEEE, pp. 119–123. <https://doi.org/10.1109/ICUMT51630.2020.9222418>.
- Tao, Z., Wang, Z., Yang, S., Shan, H., Ma, X., Zhang, H., Zhao, S., Liu, D., Xie, C., Wang, Y., 2016. Profiling the PM 2.5 mass concentration vertical distribution in the boundary layer. *Atmos. Meas. Tech.* 9, 1369–1376.
- Taseiko, O.V., Mikhailuta, S.V., Pitt, A., Lezhenin, A.A., Zakharov, Y.V., 2009. Air pollution dispersion within urban street canyons. *Atmos. Environ.* 43, 245–252. <https://doi.org/10.1016/j.atmosenv.2008.09.076>.
- Tiitta, P., Raunemaa, T., Tissari, J., Yli-Tuomi, T., Leskinen, A., Kukkonen, J., Härkönen, J., Karppinen, A., 2002. Measurements and modelling of PM2.5 concentrations near a major road in Kuopio, Finland. *Atmos. Environ.* 36, 4057–4068. [https://doi.org/10.1016/S1352-2310\(02\)00309-6](https://doi.org/10.1016/S1352-2310(02)00309-6).
- Tiwari, A., Kumar, P., Baldauf, R., Zhang, K.M., Pilla, F., Di Sabatino, S., Brattich, E., Pulvirenti, B., 2019. Considerations for evaluating green infrastructure impacts in microscale and macroscale air pollution dispersion models. *Sci. Total Environ.* 672, 410–426. <https://doi.org/10.1016/j.scitotenv.2019.03.350>.
- Trinh, Thi Thuy, Trinh, Thi Tham, Le, T.T., Nguyen, T.D.H., Tu, B.M., 2019. Temperature inversion and air pollution relationship, and its effects on human health in Hanoi City, Vietnam. *Environ. Geochem. Health* 41, 929–937. <https://doi.org/10.1007/s10653-018-0190-0>.
- US EPA, 2021. Performance testing protocols, metrics, and target values for fine particulate matter air sensors: use in ambient, outdoor, fixed site, non-regulatory supplemental and informational monitoring applications | science inventory | US EPA [WWW Document]. URL https://cfpub.epa.gov/si/si_public_record_Report.cfm?dirEntryId=350785&Lab=CEMM, 12.17.21.
- Villa, T., Gonzalez, F., Miljievic, B., Ristovski, Z., Morawska, L., 2016. An overview of small unmanned aerial vehicles for air quality measurements: present applications and future prospective. *Sensors* 16, 1072.
- Villa, T.F., Jayaratne, E.R., Gonzalez, L.F., Morawska, L., 2017. Determination of the vertical profile of particle number concentration adjacent to a motorway using an unmanned aerial vehicle. *Environ. Pollut.* 230, 134–142. <https://doi.org/10.1016/j.envpol.2017.06.033>.
- Wallace, J., Corr, D., Kanaroglou, P., 2010. Topographic and spatial impacts of temperature inversions on air quality using mobile air pollution surveys. *Sci. Total Environ.* 408, 5086–5096. <https://doi.org/10.1016/j.scitotenv.2010.06.020>.
- Wang, B., Li, Y., Tang, Z., Cai, N., Niu, H., 2021. Effects of vehicle emissions on the PM2.5 dispersion and intake fraction in urban street canyons. *J. Clean. Prod.* 324, 129212. <https://doi.org/10.1016/j.jclepro.2021.129212>.
- Wang, X., Teng, M., Huang, C., Zhou, Z., Chen, X., Xiang, Y., 2020. Canopy density effects on particulate matter attenuation coefficients in street canyons during summer in the Wuhan metropolitan area. *Atmos. Environ.* 240, 117739. <https://doi.org/10.1016/j.atmosenv.2020.117739>.
- Zheng, T., Li, B., Li, X.-B., Wang, Z., Li, S.-Y., Peng, Z.-R., 2021. Vertical and horizontal distributions of traffic-related pollutants beside an urban arterial road based on unmanned aerial vehicle observations. *Build. Environ.* 187, 107401. <https://doi.org/10.1016/j.buildenv.2020.107401>.
- Zhu, Y., Hinds, W.C., Kim, S., Sioutas, C., 2002. Concentration and size distribution of ultrafine particles near a major highway. *J. Air Waste Manag. Assoc.* 52, 1032–1042. <https://doi.org/10.1080/10473289.2002.10470842>.